A Mathematical Model Predicting Gliding Speed of Actin Molecular Shuttles Over Myosin Motors in the Presence of Defective Motors

Samuel Macharia Kang'iri(✉) and Takahiro Nitta(✉)

Gifu University, Gifu 501-1193, Japan
x3914101@edu.gifu-u.ac.jp, nittat@gifu-u.ac.jp

Abstract. Motor proteins are molecular machines that operate in living cells. These motor proteins have been used in vitro for applications such as nano- and microscale devices as transport systems in biosensors, biocomputing, and molecular communication. By introducing motor proteins into these devices, motor proteins become defective due to unfavorable binding to device surfaces, causing a decrease in transport speed or malfunctioning of transport. However, systematic experimental investigations of the effects of defective motors are hampered by difficulties in controlling the number of defective motors on surfaces. Here, we show a systematic study on the effects of defective motors on the motility of transport by using a mathematical model. The model predicted that motility is independent of the length of the associated filaments and depends on the ratio of the active motors. The model revealed that the ratio of active motors of more than 80% is required for sustainable motility. This insight would be useful in choosing appropriate materials for devices integrated with motor proteins.

Keywords: Biomolecular motor · Cytoskeleton · Biosensor

1 Introduction

Motor proteins are molecular machines that operate in living cells. These motor proteins include myosin and kinesin, which travel along the actin filament and microtubule, respectively. Through a cycle of filament binding and release, these motor proteins convert chemical energy directly to mechanical work for material transport and actuation in living cells. These motor proteins have been used in vitro for applications such as nano- and microscale devices [1]. Molecular shuttles (MS) are based on motor proteins and are essential for active transport. They have been implemented in biosensors [2–4], biocomputation [5], and molecular communication [6, 7].

As the implementation proceeds, practical problems such as the effects of defective motors arise. Defective motors, sometimes called "dead" head, ATPase catalytic domain, bind to cytoskeletal filaments but are unable to hydrolyze adenosine triphosphate (ATP), thus serving as an effective impedance to the translocation of cytoskeletal filaments driven by active motors. This causes fishtailing, swirling, and halting of the filaments [8].

T. Nakano (Ed.): BICT 2021, LNICST 403, pp. 207–214, 2021.
https://doi.org/10.1007/978-3-030-92163-7_17

While actin filament (AF) and myosin-based MS is preferable in terms of gliding speed than microtubule and kinesin-based one [9], it is more susceptible to the "dead" heads. To achieve smooth movements of AFs gliding over myosin motors in in vitro motility assay, "dead" motors have to be carefully removed prior to observation of movement, and the surfaces should be passivated to prevent "non-ideal" adhesion of myosin motors to the surface leading to denature [10]. Such coatings may not be available for use in applications since in biophysical studies, photoresists are commonly used instead of glass. Hansson *et al.* investigated the effects of various polymer materials commonly used for microfabrication on actin motility, and some fractions of myosin motors became defective depending on the nature of the polymer materials, such as hydrophobicity [11]. However, a limitation of such experimental approaches arises from the difficulty in controlling the precise amount of defective motors on surfaces, which hampers the systematic investigation.

Here, to provide predictions of gliding speed on AFs driven by myosin motors in the presence of defective motors, we developed a mathematical model. In contrast to the experimental work, the mathematical model enables a systematic quantitative investigation of the effects of defective motors on the motility of AFs. The simplicity of the mathematical model makes it easy to gain insights into the effect of defective motors.

2 Mathematical Modelling

To understand the underlying mechanism of the translocation impedance, we developed a 1D analytical model based on a previous study [12]. Our 1D model assumes that an AF is propelled by active myosin against impedance by defective ones with a gliding speed (v) (Fig. 1). The gliding speed was assumed to depend on the average force acting on each active myosin (f):

$$v = v_{max}\left(1 - \frac{f}{f_{stall}}\right) \tag{1}$$

where v_{max} is the maximum speed of the actin translocation, and f_{stall} is the stall force (-0.4 pN) [13, 14].

The acting force, f, is assumed to be exerted by the defective myosin. During the AF translocation, defective motors undergo repeated cycles of association with an AF, elongation and dissociation (Fig. 2). When an AF comes close, a defective myosin binds to the AF with a rate of $1/\tau_1$. Once bound, the defective motor is stretched by the AF translocation, building up tension impeding the AF translocation. When the tension reaches the rupture force of myosin, f_{rupt} (-9.2 pN) [15], the defective myosin dissociates from the AF. For simplicity, spontaneous dissociation of defective myosin from AF was neglected. The duration that the defective myosin binds to the AF, τ_2, depends on the AF speed and is given by $\tau_2 = -f_{rupt}/kV$, where k is the spring constant of the defective motor. Thus, the time-averaged friction force generated by a defective myosin, $\overline{f_{def}}$, is given by

$$\overline{f_{def}} = \frac{1}{\tau_1 + \tau_2}\int_0^{\tau_1+\tau_2} f_{def}\,dt. \tag{2}$$

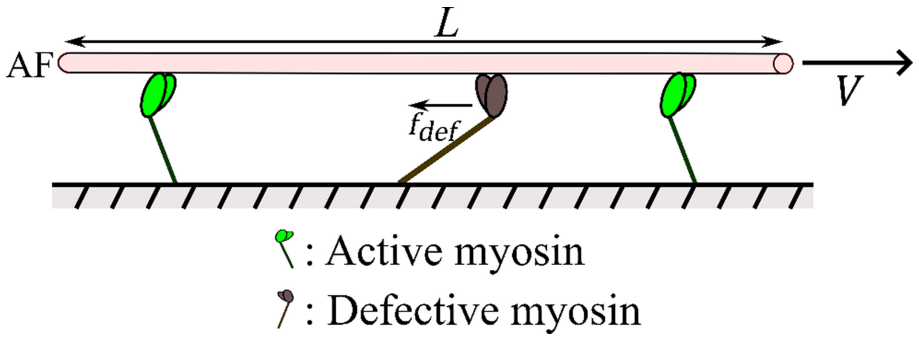

Fig. 1. A schematic drawing of actin molecular shuttles over myosin motors in the presence of defective motors.

Guided by Fig. 2, the integral can be calculated, leading to

$$\overline{f_{def}} = \frac{f_{rupt}}{2\left(1 - kv\tau_1/f_{rupt}\right)}. \tag{3}$$

Since the number of the active myosins binding to the AF with the length of L is $\rho_a L$ and that of the defective ones $\rho_d L$, where ρ_a and ρ_d are the line densities of active and defective myosins, respectively, the impedance per active myosin is given by

$$f_{imp} = \frac{\rho_d}{\rho_a} \frac{f_{rupt}}{2\left(1 - kv\tau_1/f_{rupt}\right)}. \tag{4}$$

The parameters used in this study are shown in Table 1. To obtain numerical solution, we used MATLAB.

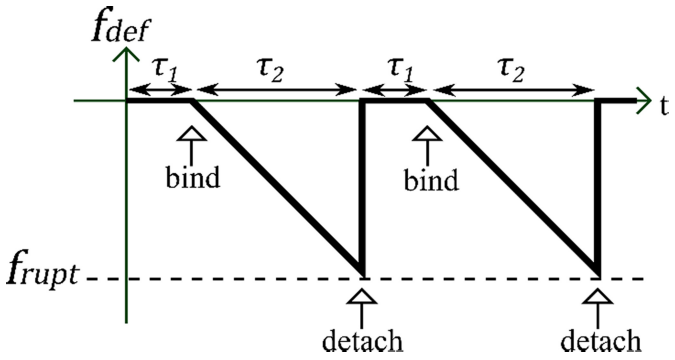

Fig. 2. A schematic representation of the time evolution of the force generated by a defective myosin.

Table 1. Parameters used

Parameter	Particulars	Value
v_{max}	Maximum gliding speed	7 μm/s
f_{stall}	Stopping/Stall force	−0.4 pN
f_{rupt}	Rupture force	−9.2 pN
k	Myosin spring constant	300 pN/μm
τ_1	Binding period	0.025

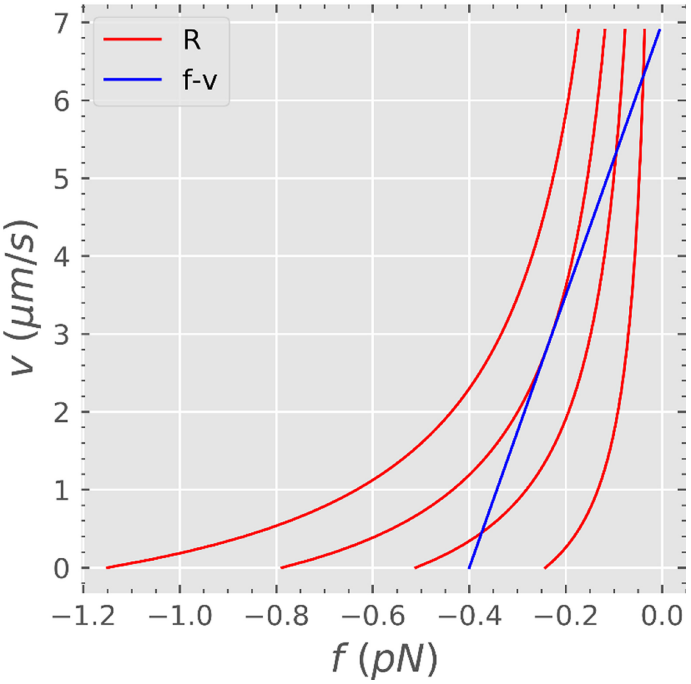

Fig. 3. A plot of the gliding speed, v, against impedance per active myosin with various active motor ratios, R (red curves), overlaid with f-v relation: Eq. (1) (blue line). The active motor ratio is 0.800, 0.854, 0.900, and 0.950 from left to right. The critical active motor ratio, in this case, was 0.854 (Color figure online).

3 Results

From Eq. (1), once the impedance is given, the AF gliding speed can be calculated. On the other hand, to determine the impedance from Eq. (3), the AF gliding is needed. Thus, to obtain the AF gliding speed, we need to solve Eqs. (1) and (3) in a self-consistent manner. That is, the gliding speed is given by the intersection of the Eqs. (1) and (3)

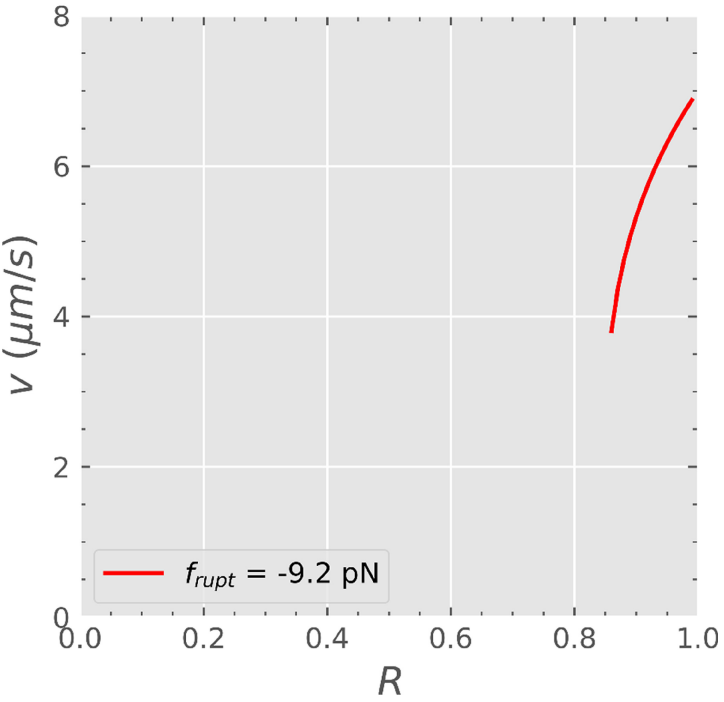

Fig. 4. The AF gliding speed, v, as a function of the active motor ratio, R.

(Fig. 3). The single parameter to determine the intersection is the gliding speed, ρ_d/ρ_a, and is independent of the length of AF.

Depending on ρ_d/ρ_a, there are three cases. At small ρ_d/ρ_a (the red curve for the active motor ratio of 0.950 in Fig. 3), there is only one solution. At an intermediate (the red curve for the active motor ratio of 0.900 in Fig. 3), there are two solutions. Above the critical value (the red curve for the active motor ratio of 0.800 in Fig. 3), there is no solution. In the case that there are two solutions, the one with the higher gliding speed is stable while the other is unstable as described below. Firstly, we consider fluctuations of the impedance around the solution with a higher gliding speed. Although we have so far discussed an averaged behavior, force fluctuation occurs due to continuous and stochastic association and dissociation of defective motors. For example, when AF happens to be decelerated by fluctuation, the impedance at this decreased speed is smaller, resulting in accelerating the AF back to the original gliding speed, showing that the solution is stable. On the other hand, around the solution with the lower gliding speed, when AF happens to be decelerated by fluctuation, the impedance at this decreased speed is larger, leading to the further deceleration of the AF, showing that the solution is unstable.

Taking the stable solutions, the gliding speed was obtained as a function of the active motor ratio, defined as $\rho_a/(\rho_a + \rho_d)$ (Fig. 4). The gliding of AFs can only occur with a rather high active motor ratio of 0.854 or more. Interestingly, due to the instability, the

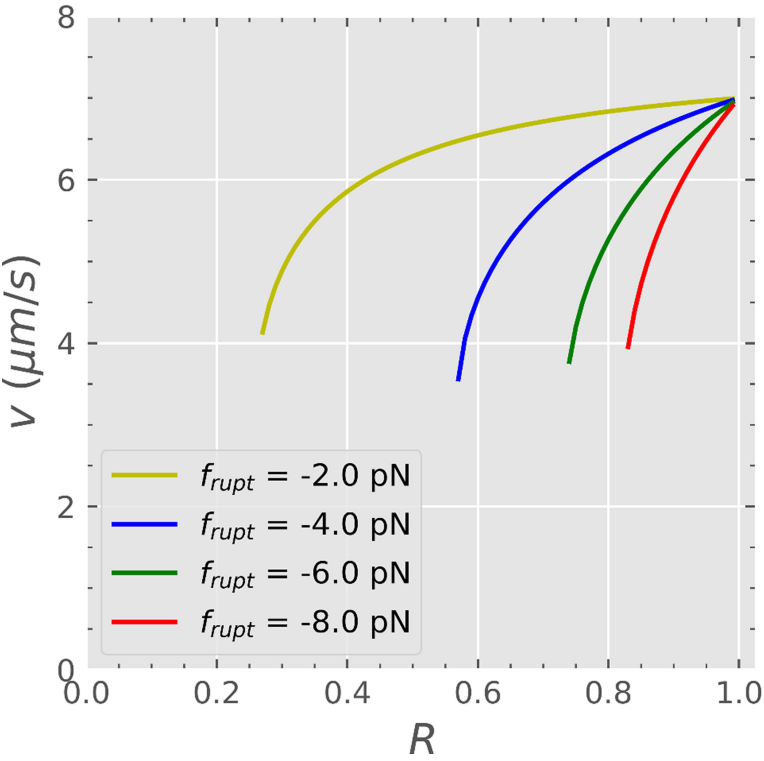

Fig. 5. The AF gliding speed as a function of the active motor ratio with various f_{rupt}.

gliding speed did not continuously increase at the onset of gliding but showed an abrupt change from 0 to 4 μm/s.

Since we neglected the spontaneous dissociation of defective myosin from AF, our choice of the rupture force of −9.2 pN may be an overestimate. We investigated the AF gliding speed as a function of the active motor ratio with various rupture forces ranging from −2.0 pN to −8.0 pN. The lower the rupture force, the lower the threshold active motor ratio for the onset of gliding movements. The abrupt change in gliding speed at the onset of motility persisted (Fig. 5).

4 Discussion

Our analytical model showed that the active motor ratio $\rho_a/(\rho_a + \rho_d)$ is the single important factor that influences the actin filament speed and that an active ratio of more than 80% is required for continuous gliding movement. The need for a high critical active motor ratio for gliding is consistent with the fact that procedures to remove defective heads are needed to achieve consistent gliding for actin/myosin in vitro motility assay.

This finding suggests that the substrate material should be carefully selected such that denaturing of the adhering myosin motors is minimized. In a study conducted by Hanson

et al. [11], higher material hydrophobicity was found to be associated with increased HMM surface adsorption but lowers the number of active HMM molecules. This study suggested that the preferable materials are those that retain the activity of motors even though the total amount of motors are limited.

The force-velocity given by Eq. (1) was employed for simplicity, which was helpful to obtain an analytical solution of the critical active motor ratio. Using a more realistic relationship such as the Hill equation [16] may yield a more accurate prediction with a drawback due to the complexity of the mathematical expression. Another shortcoming of this study would be that only 1D movements were considered. The use of computer simulation [17] would be a complementary approach to this study by dealing with 3D movements. In addition, systematic experiments with various mixing ratios of myosin and mutated defective myosin would enable qualitative validation of our mathematical model, although the exact active motor ratio would be difficult to obtain due to uncontrollable conversion of active to defective myosin.

References

1. Saper, G., Hess, H.: Synthetic systems powered by biological molecular motors. Chem. Rev. **120**(1), 288–309 (2020)
2. Lin, C.T., Kao, M.T., Kurabayashi, K., Meyhofer, E.: Self-contained, biomolecular motor-driven protein sorting and concentrating in an ultrasensitive microfluidic chip. Nano Lett. **8**(4), 1041–1046 (2008)
3. Fischer, T., Agarwal, A., Hess, H.: A smart dust biosensor powered by kinesin motors. Nat. Nanotechnol. **4**(3), 162–166 (2009)
4. Lard, M., et al.: Ultrafast molecular motor driven nanoseparation and biosensing. Biosens. Bioelectron. **48**, 145–152 (2013)
5. Nicolau, D.V., et al.: Parallel computation with molecular-motor-propelled agents in nanofabricated networks. Proc. Natl. Acad. Sci. USA **113**(10), 2591–2596 (2016)
6. Farsad, N., Yilmaz, H.B., Eckford, A., Chae, C.-B., Guo, W.: A comprehensive survey of recent advancements in molecular communication. IEEE Commun. Surv. Tutorials **18**(3), 1887–1919 (2014)
7. Nakano, T., Moore, M.J., Wei, F., Vasilakos, A.V., Shuai, J.: Molecular communication and networking: opportunities and challenges. IEEE Trans. Nanobiosci. **11**(2), 135–148 (2012)
8. Bourdieu, L., Duke, T., Elowitz, M.B., Winkelmann, D.A., Leibler, S., Libchaber, A.: Spiral defects in motility assays: a measure of motor protein force. Phys. Rev. Lett. **75**(1), 176–179 (1995)
9. Nitta, T., et al.: Comparing guiding track requirements for myosin- and kinesin-powered molecular shuttles. Nano Lett. **8**(8), 2305–2309 (2008)
10. Rahman, M.A., Salhotra, A., Månsson, A.: Comparative analysis of widely used methods to remove nonfunctional myosin heads for the in vitro motility assay. J. Muscle Res. Cell Motil. **39**(5–6), 175–187 (2019)
11. Hanson, K.L., et al.: Polymer surface properties control the function of heavy meromyosin in dynamic nanodevices. Biosens. Bioelectron. **93**, 305–314 (2017)
12. Greenberg, M.J., Moore, J.R.: The molecular basis of frictional loads in the in vitro motility assay with applications to the study of the loaded mechanochemistry of molecular motors. Cytoskeleton **67**(5), 273–285 (2010)
13. Kishino, A., Yanagida, T.: Force measurements by micromanipulation of a single actin filament by glass needles. Nature **334**(6177), 74–76 (1988)

14. Riveline, D., et al.: Acting on actin: The electric motility assay. Eur. Biophys. J. **27**(4), 403–408 (1998)
15. Nishizaka, T., Miyata, H., Yoshikawa, H., Ishiwata, S., Kinosita, K.: Unbinding force of a single motor molecule of muscle measured using optical tweezers. Nature **377**(6546), 251–254 (1995)
16. Hill, A.V.: The heat of shortening and the dynamic constants of muscle. Proc. R. Soc. London Ser. B Biol. Sci. **126**(843), 136–195 (1938)
17. Ishigure, Y., Nitta, T.: Simulating an actomyosin in vitro motility assay: toward the rational design of actomyosin-based microtransporters. IEEE Trans. Nanobiosci. **14**(6), 641–648 (2015)